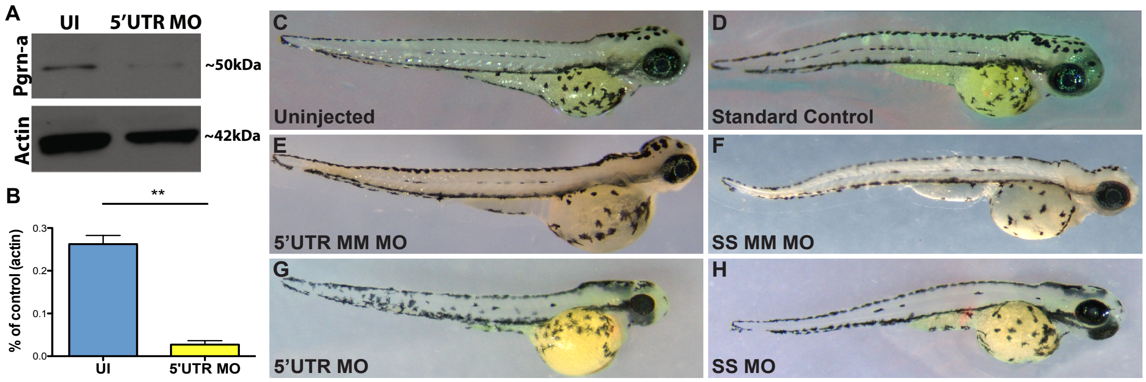

A
UI
5'UTR MO
Pgrn-a
~50kDa
Actin
~42kDa
B
**
% of control (actin)
0.3
0.2
0.1
0.0
UI
5'UTR MO
C
Uninjected
D
Standard Control
E
5'UTR MM MO
F
SS MM MO
G
5'UTR MO
H
SS MO

Figure 2.6: *pgrn-a* 5'UTR-targeting morpholinos block Pgrn-a translation and gross morphology of *pgrn-a* morphants. (A) Western blot showing Pgrn-a and Actin expression in 72hpf uninjected (UI) and morphant (5'UTR MO) embryos. **(B)** Histogram showing quantification of Pgrn-a expression in UI controls (26.2 ± 2.05%) and morphants (2.7 ± 0.9%); **$p \leq 0.01$. Quantitative data from three biological and technical replicates is normalized to Actin and represented as mean; error bars reperesent the standard deviation. **(C-H)** Representative whole embryos from control (C-F) and experimental (G-H) groups at 72hpf. 5'UTR MM MO and SS MM MO, embryos injected with 5-nucleotide mismatch control morpholinos; 5'UTR MO, embryos injected with *pgrn-a* 5'UTR-targeted morpholinos; SS MO, embryos injected with pgrn-a e3i3 splice site-targeted morpholinos.

A

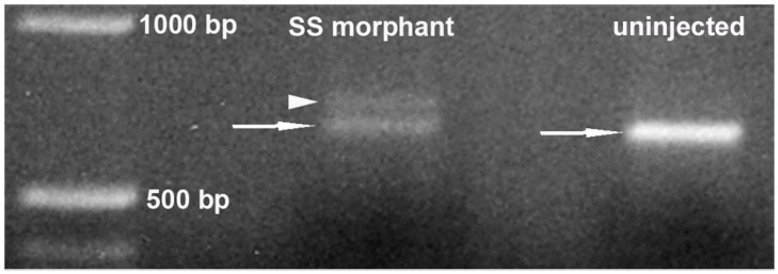

B

ATGTTGAGACTGACAGTCTGCCTCGCTGTGGTGACCCTGGTTATTTGCTCGCAGTGCCCCG
ATAATGAAGTCTGTGAAGCAGGCCAGTCCTGCTGCCAGGATCCCACTGGTGGCTTCAGCTG
CTGCCCTTTCCATCATGGAGAGTGTTGTGAAGACCATCTGCACTGCTGTCCCGAAGGCATG
TTGTGCAGTGTGAAGGACTTAACATGTACAAACGCAACACATACAGAGCCATTGGCGGACA
GGACACAAGCTAAAAAGCCAGAGTCGCCCAAAgtgagacattatatcaagcgttaagtgat
agtactcaaagctgatcgtcatgcactaataaaaacccgtttctcagTCATTCAGAATGAT
CTTCTCCATGCCTGCAAGTGAAAGCGACATCAGCTGCCCTGACGGCTCTTCCTGTCCTGCT
GAGTTCTCCTGTCTGCTGATGTCTACATCATATGGCTGCTGTCCAGTAGCACAGGGCCTTG
CATGTTCTGATGGGAAACACTGCTGCCCAAATGACCATGAATGCAGTTCTGACAGCAGCTT
GTGTGTCAACGGAAAGTAAAAGTTGAGACTGTTCTTTGTGGAAATGGGACGTCGGAGTGTC
CTGCAGACACTACATGTTGTCAGGCTGAAGATGGCCTATGGGGGTGCTGCCCCATGCCAAA
GGCTGTATGCTGTGATGACAAAATCCATTGCTGCCCAGAGGACACTGTTTGTGACGTCAAA
GCCTTGAAATGCATATCCTCAACCAACCAGAGCTGCCCATGTGGGACAAATTCCCTGCTCG
CCTTAGGGCTGAATGGGAAGATCACAAACAAAAAAAGCCTGAAACTCAACGCACTACAACT
AGACCTACAGGCACTACAAGCACTAATACAGCTGCCAACCAAATGACTACGCTGCCTGCCG
AACACCAAGCGGTGTCTTCAGATGTTCCCTGTAACGACACTGCGGCCTGTGCTGATGGA...

Figure 2.7: *pgrn-a* splice site-targeting morpholinos cause intron retention and knockdown Pgrn-a. (A) PCR confirmation of *pgrn-a* knockdown using morpholino oligonucleotides targeting the e3i3 splice site of *pgrn-a* (SS MO). The PCR product was sequenced and the double band seen in the SS morphant lane represents intron retention. The overall intensity of the Pgrna band is reduced in SS morphant when compared to uninjected control. **(B)** Sequence of *pgrn-a*. Exon sequence (upper case); intron sequence (lower case); primer sequence (blue); SS MO sequence (green); stop codon (red).

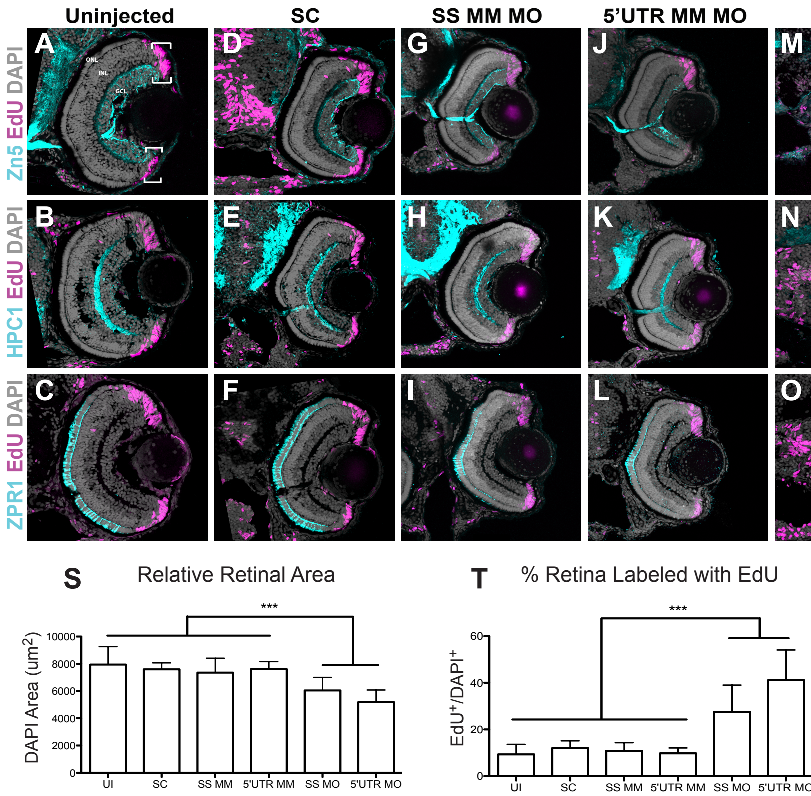

Uninjected
SC
SS MM MO
5'UTR MM MO
SS MO
5'UTR MO
Zn5 EdU DAPI
HPC1 EdU DAPI
ZPR1 EdU DAPI
A
B
C
D
E
F
G
H
I
J
K
L
M
N
O
P
Q
R
S
Relative Retinal Area
DAPI Area (um2)
UI
SC
SS MM
5'UTR MM
SS MO
5'UTR MO
T
% Retina Labeled with EdU
EdU+/DAPI+

Figure 2.8: Pgrn-a knockdown results in microphthalmia and diminished neuronal differentiation. (A-R) Sections through central retina of uninjected (UI, A-C); standard control morpholino-injected (SC, D-F); SS MM (G-I) and 5'UTR MM (J-L), embryos injected with 5-nucleotide mismatch control morpholinos; SS MO (M-O) and 5'UTR MO (P-R), embryos injected with e3i3 splice site-targeted or 5'UTR-targeted morpholinos, respectively, at 72hpf. Sections are immunolabeled (cyan) with markers of differentiated ganglion cells (Zn5, top row), amacrine cells (HPC1, middle row), and red-green double cone photoreceptor cells (ZPR1, bottom row), EdU (fusia), and DAPI (gray). **(S)** Histogram showing relative retinal area in UI (7945.8 ± 1319.6 μm^2; *n*=11), SC-injected (7594.3 ± 475.2 μm^2; *n*=9), SS MM MO-injected (7354 ± 1062.6 μm^2; *n*=11), and 5'UTR MM MO-injected (7610.8 ± 547.6 μm^2; *n*=10), SS MO (6044.7 ± 956.2 μm^2; *n*=10), and 5'UTR MO (5188.7 ± 891.8 μm^2; *n*=16) retinas at 72hpf; ***p≤0.001. **(T)** Histogram showing the percent of the retina labeled with EdU in UI (9.3 ± 4.3%; *n*=11), SC-injected (12 ± 3.1%; *n*=9), SS MM MO-injected (10.8 ± 3.5%; *n*=11), 5'UTR MM MO-injected (9.8 ± 2.3%; *n*=10), SS MO-injected (27.5 ± 11.5%; *n*=10), and 5'UTR MO-injected (41.1 ± 13%; *n*=16) retinas at 72hpf; ***p≤0.001. Quantitative data are represented as mean; error bars reperesent the standard deviation. Outer nuclear layer (ONL), inner nuclear layer (INL), and ganglion cell layer (GCL); ciliary marginal zone (CMZ, brackets). Scale bar equals 50µm.

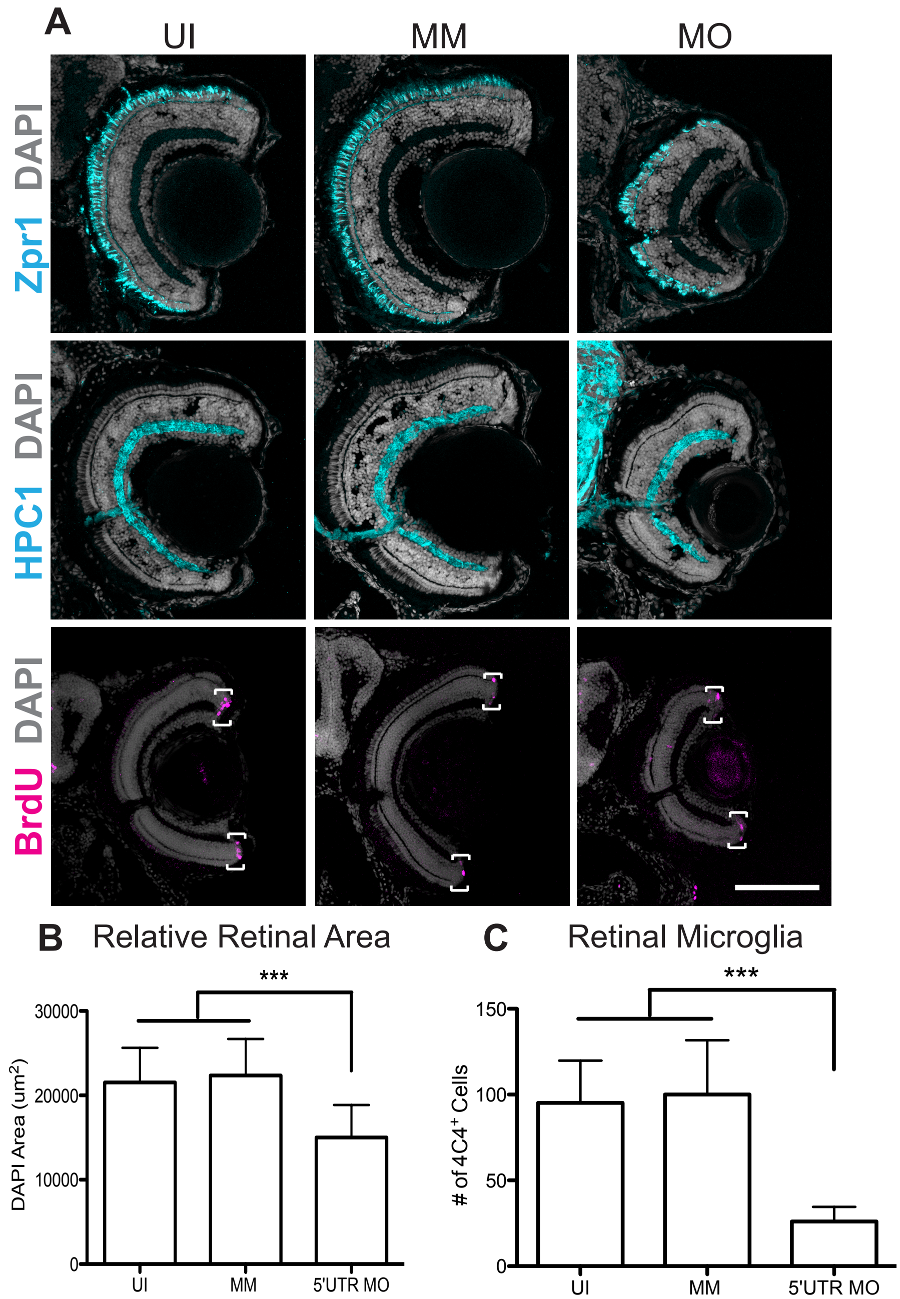
A
UI
MM
MO
Zpr1 DAPI
HPC1 DAPI
BrdU DAPI
B
Relative Retinal Area
***
DAPI Area (um^2)
30000
20000
10000
0
UI
MM
5'UTR MO
C
Retinal Microglia
***
# of 4C4$^+$ Cells
150
100
50
0
UI
MM
5'UTR MO

Figure 2.9: Aspects of Pgrn-a knockdown retinal phenotype recover by 8dpf. (A) Sections through central retina of uninjected (UI, left column), 5'UTR MM MO (middle column), and 5'UTR MO (right column) larvae at 8dpf, immunolabeled (cyan) with markers of red-green cone photoreceptors (ZPR1, top row) and amacrine cells (HCP1, middle row), BrdU (fusia, bottom row), and DAPI (gray). **(B)** Histogram showing the size of the retina in UI (21533.35 ± 4112.8 μm^2; *n*=15), 5'UTR MM MO (22360.0 ± 4324.0 μm^2; *n*=9), and 5'UTR MO (15000.4 ± 3861.2 μm^2; *n*=15) larvae at 8dpf; ***p<0.001. **(C)** Histogram showing the number of retinal microglia ($4C4^+$ cells) in UI (95.2 ± 24.7 cells; *n*=15), 5'UTR MM MO (100 ± 31.7 cells; *n*=9), and 5'UTR MO (26.1 ± 8.5 cells; *n*=15) larvae at 8dpf; ***p<0.001. Quantitative data are represented as mean; error bars reperesent the standard deviation. Outer nuclear layer (ONL), inner nuclear layer (INL), and ganglion cell layer (GCL). Scale bar equals 100µm.

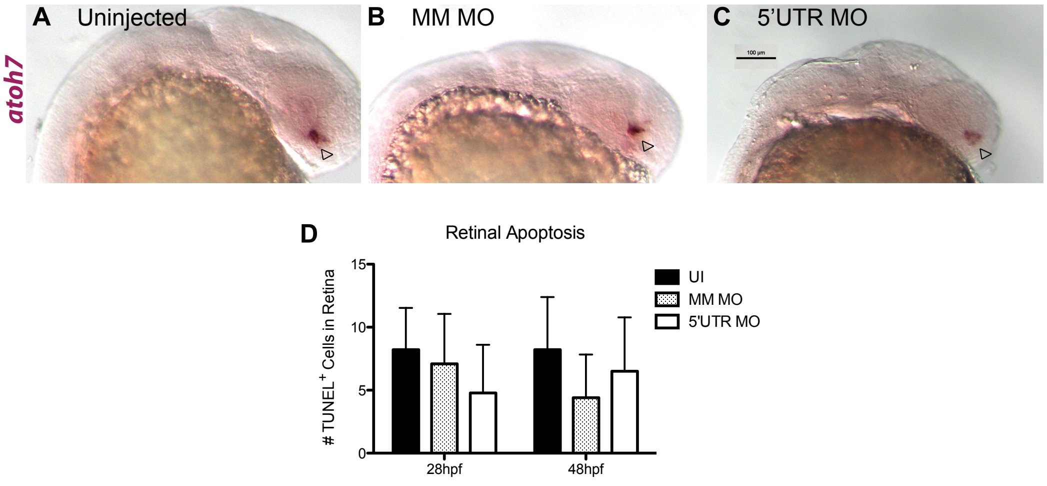
A
Uninjected
B
MM MO
C
5'UTR MO
atoh7
100 μm
D
Retinal Apoptosis
TUNEL+ Cells in Retina
15
10
5
0
28hpf
48hpf
UI
MM MO
5'UTR MO

Figure 2.10: No difference in *atoh7* expression and TUNEL-positive cell counts between *pgrn-a* morphant and control embryos. Whole mount *in situ* hybridization showing *atoh7* expression in uninjected **(A)**, 5'UTR MM MO **(B)**, and 5'UTR MO **(C)** embryos at 28hpf. **(D)** Histogram showing the number of TUNEL-positive cells in uninjected, 5'UTR MM MO-injected, and 5'UTR MO-injected retinas at 28 and 48hpf.

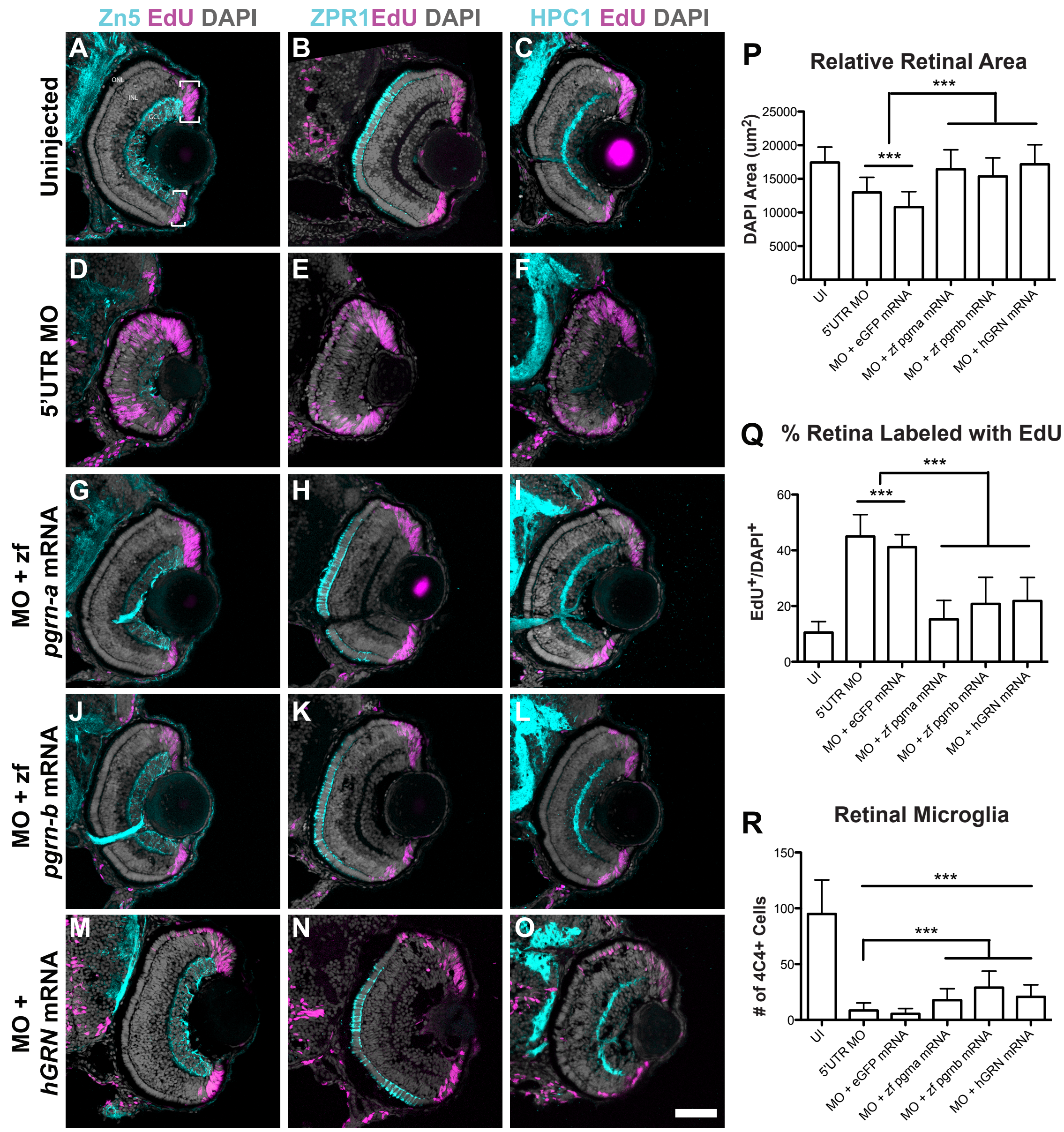
Zn5 EdU DAPI
ZPR1EdU DAPI
HPC1 EdU DAPI
A
B
C
Uninjected
D
E
F
5'UTR MO
G
H
I
MO + zf pgrn-a mRNA
J
K
L
MO + zf pgrn-b mRNA
M
N
O
MO + hGRN mRNA
P
Relative Retinal Area
DAPI Area (um2)
25000
20000
15000
10000
5000
0
***
***
UI
5'UTR MO
MO + eGFP mRNA
MO + zf pgrna mRNA
MO + zf pgrnb mRNA
MO + hGRN mRNA
Q
% Retina Labeled with EdU
EdU+/DAPI+
60
40
20
0
***
***
R
Retinal Microglia
# of 4C4+ Cells
150
100
50
0
***
***

Figure 2.11: Co-injection of 5'UTR MO and zf *pgrn-a*, zf *pgrn-b*, or *hGRN* mRNA rescues most aspects of knockdown retinal phenotype. (A-O) Cross-sections through central retina of 72hpf uninjected (UI, A-C), 5'UTR MO-injected (D-F), 5'UTR MO and zf *pgrn-a* mRNA co-injected (G-I), 5'UTR MO and zf *pgrn-b* mRNA co-injected (J-L), and 5'UTR MO and *hGRN* mRNA co-injected (M-O) embryos at 72 hpf. Sections are immunolabeled (cyan) with markers for ganglion cells (Zn-5, left column), red-green double cone photoreceptors (Zpr1, middle column), and amacrine cells (HPC1, right column), EdU (fusia), and DAPI (gray). **(P)** Histogram showing relative retinal area of UI (17437.4 ± 2286.1 μm^2; *n*=23), 5'UTR MO-injected (12961.2 ± 2251.8 μm^2; *n*=21), 5'UTR MO and *eGFP* mRNA co-injected (10809 ± 2282.5 μm^2; *n*=8), 5'UTR MO and zf *pgrn-a* mRNA co-injected (16435.7 ± 2882.2 μm^2; *n*=12), 5'UTR MO and zf *pgrn-b* mRNA co-injected (15357.8 ± 2750.2 μm^2; *n*=13), and 5'UTR MO and *hGRN* mRNA co-injected (17146.1 ± 2930.7 μm^2; *n*=12) embryos at 72hpf; ***p<0.001. **(Q)** Histogram showing the percent of the retina labeled with EdU in UI (10.5 ± 3.9%; *n*=7), 5'UTR MO-injected (45 ± 7.9%; *n*=18), 5'UTR MO and *eGFP* mRNA co-injected (41.1 ± 4.5%; *n*=6), 5'UTR MO and zf *pgrn-a* mRNA co-injected (15.2 ± 6.8%; *n*=22), 5'UTR MO and zf *pgrn-b* mRNA co-injected (20.8 ± 9.6%; *n*=18), and 5'UTR MO and *hGRN* mRNA co-injected (21.8 ± 8.5%; *n*=12) embryos at 72hpf; ***p<0.001. **(R)** Histogram showing the number of retinal microglia ($4C4^+$ cells) at 72hpf in UI (95 ± 30.5 cells; *n*=23), 5'UTR MO-injected (8.4 ± 6.8 cells; *n*=21), 5'UTR MO and *eGFP* mRNA co-injected (5.4 ± 4.8 cells; *n*=8), 5'UTR MO and zf *pgrn-a* mRNA co-injected (17.7 ± 10.2 cells; *n*=12), 5'UTR MO and zf *pgrn-b* mRNA co-injected (28.9 ± 14.7 cells; *n*=13), and 5'UTR MO and *hGRN* mRNA co-injected (20.6 ± 10.8; *n*=12) embryos; ***p<0.001. Quantitative data are represented as mean; error bars reperesent the standard deviation. Outer nuclear layer (ONL), inner nuclear layer (INL), and ganglion cell layer (GCL); ciliary marginal zone (CMZ, brackets). Scale bar equals 50μm.

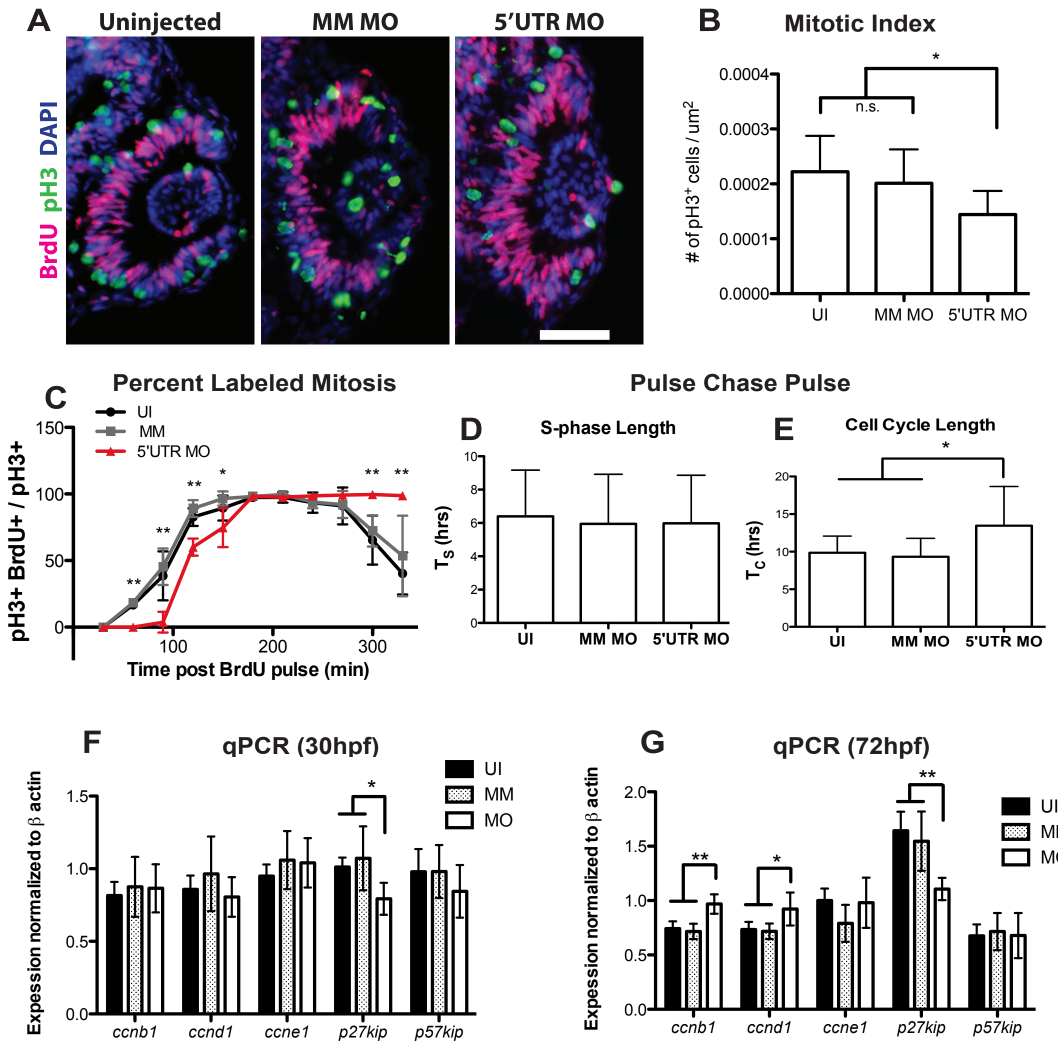

A
Uninjected
MM MO
5′UTR MO
BrdU pH3 DAPI
B
Mitotic Index
# of pH3+ cells / um2
0.0004
0.0003
0.0002
0.0001
0.0000
n.s.
*
UI
MM MO
5'UTR MO
C
Percent Labeled Mitosis
UI
MM
5'UTR MO
pH3+ BrdU+ / pH3+
Time post BrdU pulse (min)
Pulse Chase Pulse
D
S-phase Length
E
Cell Cycle Length
F
qPCR (30hpf)
Expression normalized to β actin
ccnb1
ccnd1
ccne1
p27kip
p57kip
G
qPCR (72hpf)

Figure 2.12: Knockdown of *pgrn-a* alters cell cycle kinetics in retinal progenitors. **(A)** Representative retinal sections from 28hpf uninjected (left panel), MM MO (center panel), and 5'UTR MO (right panel) embryos stained with antibodies against pH3 (green), BrdU (fusia), and DAPI (blue) used for quantification of mitotic index. **(B)** Histogram showing the mitotic index at 28hpf. The number of $pH3^+$ cells/unit area in UI (0.0002 ± 1.973e-005 cells per μm^2; *n*=11), MM MO (0.0002 ± 1.947e-005 cells per μm^2; *n*=10), and 5'UTR MO retinas (0.0001 ± 1.366e-005 cells per μm^2; *n*=10); *p≤0.01. **(C)** Graph showing the percent labeled mitosis for UI, MM MO and 5'UTR MO embryos between 28 and 35hpf. **(D)** Histogram showing average S-phase length (T_S) in 26-28hpf UI (6.4 ± 2.8hrs; *n*=16), MM MO (5.9 ± 3.0hrs; *n*=10), and 5'UTR MO (6.0 ± 2.9hrs; *n*=7) embryos. **(E)** Histogram showing average total cell cycle length (T_C) at 26-28hpf in UI (9.9 ± 2.2hrs; *n*=16), MM MO (9.3 ± 2.5hrs; *n*=10), and 5'UTR MO (13.5 ± 5.2hrs; *n*=7); *p≤0.05. **F-G)** Histograms showing relative cyclin B (*ccnb1*), cyclin D (*ccnd1*), cyclin E (*ccne1*), *p27kip* and *p57kip* mRNA expression normalized to beta actin at 30hpf (F) and 72hpf (G); *p≤0.05 and **p≤0.01. Quantitative data are represented as mean; error bars reperesent the standard deviation. Scale bar = 50μm.

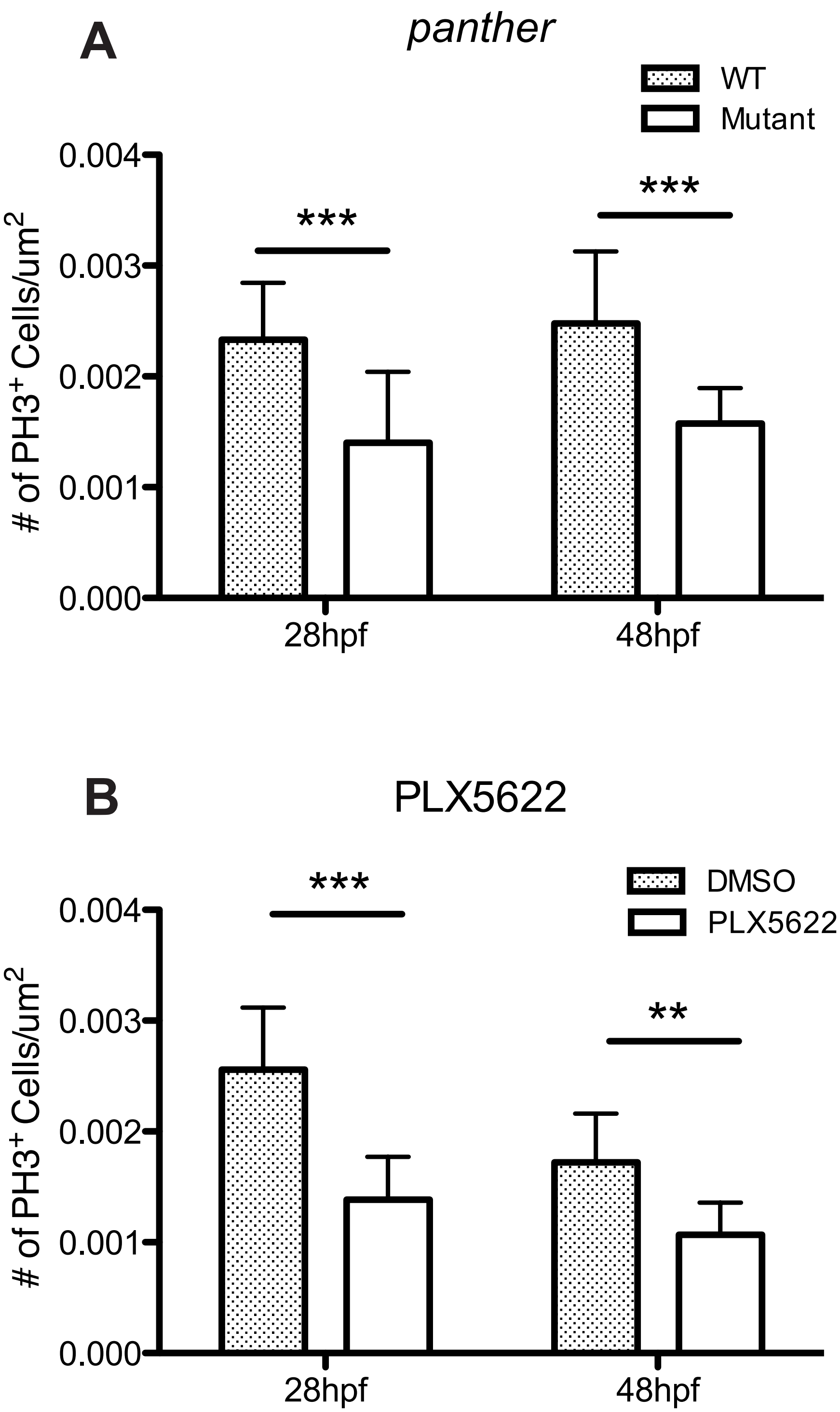
A
panther
WT
Mutant
***
***
# of PH3+ Cells/um2
0.004
0.003
0.002
0.001
0.000
28hpf
48hpf
B
PLX5622
DMSO
PLX5622
***
**
# of PH3+ Cells/um2
0.004
0.003
0.002
0.001
0.000
28hpf
48hpf

Figure 2.13: Mitotic index in 28 and 48hpf panther mutant and PLX5622-treated embryos. (A) Histogram showing the ratio of $pH3^+$ cells in wild type (WT; .002 ± .0005 cells per μm^2; *n*=14) and *panther* mutant (.001 ± .0006 cells per μm^2; *n*=22) retinas at 28hpf and in WT (.002 ± .0006 cells per μm^2; *n*=12) and *panther* mutant (.002 ± .0003 cells per μm^2; *n*=18) retinas at 48hpf; ***p≤0.001. **(B)** Histogram showing the ratio of $pH3^+$ cells in DMSO-treated control (.003 ± .0006 cells per μm^2; *n*=11) and PLX5622-treated (.001 ± .0004 cells per μm^2; *n*=12) retinas at 28hpf, and DMSO-treated control (.002 ± .0004 cells per μm^2; *n*=10) and PLX5622-treated (.001 ± .0003 cells per μm^2; *n*=10) retinas at 48hpf; ***p≤0.001. Quantitative data are represented as mean; error bars reperesent the standard deviation.

Table 2.1: Antibody List

Primary Antibodies	Company	Dilution
Monoclonal anti-Zn5	ZIRC; zfin.org/ZDB-ATB-081002-19	1:200
Monoclonal anti-Zpr1 (anti-Arrestin)	ZIRC; zfin.org/ZDB-ATB-081002-43	1:200
Mouse anti-HPC1 (anti-Syntaxin)	Sigma S0664	1:200
Monoclonal anti-4C4	Umich Hybridoma Core	1:200
Rabbit anti-leucocyte-specific plastin (L-plastin)	Gift from Michael Redd	1:500
Mouse anti-BrdU	BD Biosciences 347580	1:100
Rabbit anti-pH3 (phospho-histone 3 ser10)	Millipore 06-570	1:200
Secondary Antibodies		
Alexa Fluor goat anti-mouse 488 or 555	Invitrogen	1:500
Alexa Fluor goat anti-rabbit 488 or 555	Invitrogen	1:500

Table 2.2: Restriction Enzymes and RNA Polymerases for *pgrn-a*, *atoh7*, and *fms* Riboprobe Synthesis

Probe	Restriction Enzyme	RNA polymerase
pgrn-a sense	SalI	T7
pgrn-a anti-sense	SmaI	T3
atoh7 anti-sense	EcoRI	T7
fms anti-sense	EcoRI	T7

Table 2.3: Morpholino Oligonucleotide Sequences

Name	Sequence
pgrn-a 5'UTR MO	5'-AGCGGAAAGTAAATGATCAGTCCGT-3'
pgrn-a 5'UTR MM MO	5'-AGCGcAAAcTAtATcATCAcTCCGT-3'
pgrn-a SS MO	5'-TATAATGTCTCACTTTGGGAAGGTC-3'
pgrn-a SS MM MO	5'-TAaAATcTCTgACTTaGcGAAGGTC-3'
fms MO	5'-AAGAGCGCGAAGAACATCTCAGAGC-3'
fms MM MO	5'-AAcAcCGCcAAcAACATCTCAcAGC-3'
p53 MO	5'-GCGCCATTGCTTTGCAAGAATTG-3'
SC MO	5'-CCTCTTACCTCAGTTACAATTTATA-3'

Table 2.4: Primer Sequences for mRNA Rescue Experiments

Primer Name	Sequence
zf_pgrna_FW	ATGTTGAGACTGACAGTCTGCC
zf_pgrna_REV	TTATAGAGTTAGGGCTCGTTTC
zf_pgrnb_FW	ATGGTGCGTGCAGCTTTCATAGC
zf_pgrnb_REV	TTAGAGAGAATTATTCCACCACG

Table 2.5: Primer Sequences for qRT-PCR

Gene	Forward Primer	Reverse Primer
cycB1	AGTTTAGGCTGCTTCAGGAGAC	ATGCACGGTCTGTCACAAAAGC
cycD1	CAAACACGCCCAGACCTTTGTG	GGGTCACTTCTGATGACTTGCG
cycE1	GGAAGAGAAAAGCAGACGTGGC	GGTTCCTCGACTTCATCAGGTG
p27kip	AACGGGAATCACGACTGTAGGG	ATGTGGGTGTCGGACTCAATGG
p57kip	CCGGTAGCTCAAGAATCCGAGG	TCGTGGATGTGCCGGCTTGAAG
bactin	GCAATGAGCGTTTCCGTTG	TGTGTTGGCATACAGGTCC

REFERENCES

Agathocleous M, Harris WA. 2009. From Progenitors to Differentiated Cells in the Vertebrate Retina. Annu Rev Cell Dev Biol 25:45–69.

Asakura R, Matsuwaki T, Shim J-H, Yamanouchi K, Nishihara M. 2011. Involvement of progranulin in the enhancement of hippocampal neurogenesis by voluntary exercise. Neuroreport 22:881–886.

Baker M, Mackenzie IR, Pickering-Brown SM, Gass J, Rademakers R, Lindholm C, Snowden J, Adamson J, Sadovnick AD, Rollinson S, Cannon A, Dwosh E, Neary D, Melquist S, Richardson A, Dickson D, Berger Z, Eriksen J, Robinson T, Zehr C, Dickey CA, Crook R, McGowan E, Mann D, Boeve B, Feldman HH, Hutton M. 2006. Mutations in progranulin cause tau-negative frontotemporal dementia linked to chromosome 17. Nature 442:916–919.

Bateman A, Bennett HP. 1998. Granulins: the structure and function of an emerging family of growth factors. J Endocrinol 158:145–151.

Bateman A, Bennett HPJ. 2009. The granulin gene family: from cancer to dementia. Bioessays 31:1245–1254.

Baye LM, Link BA. 2007. Interkinetic nuclear migration and the selection of neurogenic cell divisions during vertebrate retinogenesis. J Neurosci 27:10143–10152.

Bilimoria PM, Stevens B. 2014. Microglia function during brain development: New insights from animal models. Brain Research.

Bill BR, Petzold AM, Clark KJ, Schimmenti LA, Ekker SC. 2009. A Primer for Morpholino Use in Zebrafish. Zebrafish 6:69–77.

Butovsky O, Ziv Y, Schwartz A, Landa G, Talpalar AE, Pluchino S, Martino G, Schwartz M. 2006. Microglia activated by IL-4 or IFN-γ differentially induce neurogenesis and oligodendrogenesis from adult stem/progenitor cells. Molecular and Cellular Neuroscience 31:149–160.

Cadieux B, Chitramuthu BP, Baranowski D, Bennett HP. 2005. The zebrafish progranulin gene family and antisense transcripts. BMC Genomics 6:156.

Cepko CL, Austin CP, Yang X, Alexiades M, Ezzeddine D. 1996. Cell fate determination in the vertebrate retina. Proceedings of the National Academy of Sciences of the United States of America 93:589–595.

Craig SEL, Calinescu A-A, Hitchcock PF. 2008. Identification of the molecular signatures integral to regenerating photoreceptors in the retina of the zebra fish. j ocul biol dis inform 1:73–84.

Cruts M, Gijselinck I, van der Zee J, Engelborghs S, Wils H, Pirici D, Rademakers R, Vandenberghe R, Dermaut B, Martin J-J, van Duijn C, Peeters K, Sciot R, Santens P, De Pooter T, Mattheijssens M, Van den Broeck M, Cuijt I, Vennekens K, De Deyn PP, Kumar-Singh S, Van Broeckhoven C. 2006. Null mutations in progranulin cause ubiquitin-positive frontotemporal dementia linked to chromosome 17q21. Nature 442:920–924.

Cuadros MA, Martin C, Coltey P, Almendros A, Navascués J. 1993. First appearance, distribution, and origin of macrophages in the early development of the avian central nervous system. J Comp Neurol 330:113–129.

Cuadros MA, Navascués J. 2001. Early origin and colonization of the developing central nervous system by microglial precursors. Prog Brain Res 132:51–59.

Cunningham CL, Martinez-Cerdeno V, Noctor SC. 2013. Microglia Regulate the Number of Neural Precursor Cells in the Developing Cerebral Cortex. Journal of Neuroscience 33:4216–4233.

Dai X-M, Zong X-H, Akhter MP, Stanley ER. 2004. Osteoclast deficiency results in disorganized matrix, reduced mineralization, and abnormal osteoblast behavior in developing bone. J Bone Miner Res 19:1441–1451.

Daniel R, He Z, Carmichael KP, Halper J, Bateman A. 2000. Cellular localization of gene expression for progranulin. J Histochem Cytochem 48:999–1009.

Das T, Payer B, Cayouette M, Harris WA. 2003. In vivo time-lapse imaging of cell divisions during neurogenesis in the developing zebrafish retina. Neuron 37:597–609.

De I, Nikodemova M, Steffen MD, Sokn E, Maklakova VI, Watters JJ, Collier LS. 2014. CSF1 overexpression has pleiotropic effects on microglia in vivo. Glia 62:1955–1967.

De Muynck L, Van Damme P. 2011. Cellular Effects of Progranulin in Health and Disease. J Mol Neurosci.

Del Rio Hortega P. 1939. THE MICROGLIA. The Lancet Neurology [Internet]. Available from: http://www.sciencedirect.com/science/article/pii/S0140673600605718

Dong T, Yang D, Li R, Zhang L, Zhao H, Shen Y, Zhang X, Kong B, Wang L. 2015. Experimental and Molecular Pathology:1–27.

Easter SS, Nicola GN. 1996. The development of vision in the zebrafish (Danio rerio). Developmental Biology 180:646–663.

Eisen JS, Smith JC. 2008. Controlling morpholino experiments: don't stop making antisense. Development 135:1735–1743.

Elmore MRP, Najafi AR, Koike MA, Dagher NN, Spangenberg EE, Rice RA, Kitazawa M, Matusow B, Nguyen H, West BL, Green KN. 2014. Colony-Stimulating Factor 1 Receptor Signaling Is Necessary for Microglia Viability, Unmaskinga Microglia Progenitor Cell in the Adult Brain. Neuron 82:380–397.

Erblich B, Zhu L, Etgen AM, Dobrenis K, Pollard JW. 2011. PLOS ONE: Absence of Colony Stimulation Factor-1 Receptor Results in Loss of Microglia, Disrupted Brain Development and Olfactory Deficits. PLoS ONE [Internet] 6:e26317. Available from: http://journals.plos.org/plosone/article?id=10.1371/journal.pone.0026317

Fischer AJ, Zelinka C, Gallina D, Scott MA, Todd L. 2014. Reactive microglia and macrophage facilitate the formation of Müller glia-derived retinal progenitors. Glia 62:1608–1628.

Gao X, Joselin AP, Wang L, Kar A, Ray P, Bateman A, Goate AM, Wu JY. 2010. Progranulin promotes neurite outgrowth and neuronal differentiation by regulating GSK-3β. Protein Cell 1:552–562.

Garden GA, Möller T. 2006. Microglia biology in health and disease. J Neuroimmune Pharmacol 1:127–137.

Ginhoux F, Greter M, Leboeuf M, Nandi S, See P, Gokhan S, Mehler MF, Conway SJ, Ng LG, Stanley ER, Samokhvalov IM, Merad M. 2010. Fate Mapping Analysis Reveals That Adult Microglia Derive from Primitive Macrophages. Science 330:841–845.

Ginhoux F, Prinz M. 2015. Origin of Microglia: Current Concepts and Past Controversies. Cold Spring Harbor Perspectives in Biology 7.

Gramage E, D'Cruz T, Taylor S, Thummel R, Hitchcock PH. 2015. Midkine-a Protein Localization in the Developing and Adult Retina of the Zebrafish and Its Function During Photoreceptor Regeneration. PLoS ONE 10.

Haidi Zhang GS. 1998. Inhibition of tumorigenicity of the teratoma PC cell line by transfection with antisense cDNA for PC cell-derived growth factor (PCDGF, epithelin/granulin precursor). Proceedings of the National Academy of Sciences of the United States of America 95:14202.

Hanisch U-K, Kettenmann H. 2007. Microglia: active sensor and versatile effector cells in the normal and pathologic brain. Nat Neurosci 10:1387–1394.

He Z, Bateman A. 1999. Progranulin gene expression regulates epithelial cell growth and promotes tumor growth in vivo. Cancer Res 59:3222–3229.

He Z, Bateman A. 2003. Progranulin (granulin-epithelin precursor, PC-cell-derived growth factor, acrogranin) mediates tissue repair and tumorigenesis. Journal of Molecular Medicine 81:600–612.

He Z, Ismail A, Kriazhev L, Sadvakassova G, Bateman A. 2002. Progranulin (PC-Cell-derived Growth Factor/Acrogranin) Regulates Invasion and Cell Survival. Cancer Res 62:5590 –5596.

He Z, Ong CHP, Halper J, Bateman A. 2003. Progranulin is a mediator of the wound response. Nat Med 9:225–229.

Herbomel P, Levraud J-P. 2005. Imaging early macrophage differentiation, migration, and behaviors in live zebrafish embryos. Methods Mol Med 105:199–214.

Herbomel P, Thisse B, Thisse C. 1999. Ontogeny and behaviour of early macrophages in the zebrafish embryo. Development 126:3735–3745.

Herbomel P. 2001. Zebrafish Early Macrophages Colonize Cephalic Mesenchyme and Developing Brain, Retina, and Epidermis through a M-CSF Receptor-Dependent Invasive Process. Developmental Biology 238:274–288.

Hitchcock P, Kakuk-Atkins L. 2004. The basic helix-loop-helix transcription factor neuroD is expressed in the rod lineage of the teleost retina. J Comp Neurol 477:108–117.

Hitchcock P, Ochocinska M, Sieh A, Otteson D. 2004. Persistent and injury-induced neurogenesis in the vertebrate retina. Prog Retin Eye Res 23:183–194.

Hitchcock PF, Raymond PA. 2004. The teleost retina as a model for developmental and regeneration biology. Zebrafish 1:257–271.

Hu M, Easter SS. 1999. Retinal neurogenesis: the formation of the initial central patch of postmitotic cells. Developmental Biology 207:309–321.

Kay JN. 2005. Staggered cell-intrinsic timing of ath5 expression underlies the wave of ganglion cell neurogenesis in the zebrafish retina. Development 132:2573–2585.

Kettenmann H, Hanisch UK, Noda M, Verkhratsky A. 2011. Physiology of Microglia. Physiological Reviews 91:461–553.

Kok FO, Shin M, Ni C-W, Gupta A, Grosse AS, van Impel A, Kirchmaier BC, Peterson-Maduro J, Kourkoulis G, Male I, DeSantis DF, Sheppard-Tindell S, Ebarasi L, Betsholtz C, Schulte-Merker S, Wolfe SA, Lawson ND. 2015. Reverse Genetic Screening RevealsPoor Correlation between Morpholino-Induced and Mutant Phenotypes in Zebrafish. Developmental Cell 32:97–108.

Li YH, Chen MHC, Gong HY, Hu SY, Li YW, Lin GH, Lin CC, Liu W, Wu JL. 2010. Progranulin A-mediated MET Signaling Is Essential for Liver Morphogenesis in Zebrafish. Journal of Biological Chemistry 285:41001–41009.

Li Z, Hu M, Ochocinska MJ, Joseph NM, Easter SS. 2000. Modulation of cell proliferation in the embryonic retina of zebrafish (Danio rerio). Dev Dyn 219:391–401.

Liau LM, Lallone RL, Seitz RS, Buznikov A, Gregg JP, Kornblum HI, Nelson SF, Bronstein JM. 2000. Identification of a human glioma-associated growth factor gene, granulin, using differential immuno-absorption. Cancer Res 60:1353–1360.

Luo J, Uribe RA, Hayton S, Calinescu A-A, Gross JM, Hitchcock PF. 2012. Midkine-A functions upstream of Id2a to regulate cell cycle kinetics in the developing vertebrate retina. Neural Development 7:33.

Mara E Robu JDLANSBCBSAF, Ekker SC. 2007. p53 Activation by Knockdown Technologies. PLoS Genet 3:e78–15.

Masai I, Stemple DL, Okamoto H, Wilson SW. 2000. Midline signals regulate retinal neurogenesis in zebrafish. Neuron 27:251–263.

Meireles AM, Shiau CE, Guenther CA, Sidik H, Kingsley DM, Talbot WS. 2014. The phosphate exporter xpr1b is required for differentiation of tissue-resident macrophages. Cell Rep 8:1659–1667.

Moisse K, Volkening K, Leystra-Lantz C, Welch I, Hill T, Strong MJ. 2009. Divergent patterns of cytosolic TDP-43 and neuronal progranulin expression following axotomy: Implications for TDP-43 in the physiological response to neuronal injury. Brain Research 1249:202–211.

Monami G, Gonzalez EM, Hellman M, Gomella LG, Baffa R, Iozzo RV, Morrione A. 2006. Proepithelin promotes migration and invasion of 5637 bladder cancer cells through the activation of ERK1/2 and the formation of a paxillin/FAK/ERK complex. Cancer Res 66:7103–7110.

Morgan SC, Taylor DL, Pocock JM. 2004. Microglia release activators of neuronal proliferation mediated by activation of mitogen-activated protein kinase, phosphatidylinositol-3-kinase/Akt and delta-Notch signalling cascades. J Neurochem 90:89–101.

Nandi S, Gokhan S, Dai X-M, Wei S, Enikolopov G, Lin H, Mehler MF, Stanley ER. 2012. The CSF-1 receptor ligands IL-34 and CSF-1 exhibit distinct developmental brain expression patterns and regulate neural progenitor cell maintenance and maturation. Developmental Biology 367:100–113.

Naphade SB, Kigerl KA, Jakeman LB, Kostyk SK, Popovich PG, Kuret J. 2009. Progranulin expression is upregulated after spinal contusion in mice. Acta Neuropathol 119:123–133.

Nasevicius A, Ekker SC. 2000. Effective targeted gene “knockdown” in zebrafish.

Nat Genet 26:216–220.

Nayak D, Roth TL, McGavern DB. 2014. Microglia development and function. Annu Rev Immunol 32:367–402.

Nedachi T, Kawai T, Matsuwaki T, Yamanouchi K, Nishihara M. 2011. Progranulin enhances neural progenitor cell proliferation through glycogen synthase kinase 3β phosphorylation. Neuroscience 185:106–115.

Nikolakopoulou AM, Dutta R, Chen Z, Miller RH, Trapp BD. 2013. Activated microglia enhance neurogenesis via trypsinogen secretion. Proceedings of the National Academy of Sciences 110:8714–8719.

Nimmerjahn A. 2005. Resting Microglial Cells Are Highly Dynamic Surveillants of Brain Parenchyma in Vivo. Science 308:1314–1318.

Ninkovic J, Götz M. 2007. Signaling in adult neurogenesis: from stem cell niche to neuronal networks. Current Opinion in Neurobiology 17:338–344.

Ochocinska MJ, Hitchcock PF. 2007. Dynamic expression of the basic helix-loop-helix transcription factor neuroD in the rod and cone photoreceptor lineages in the retina of the embryonic and larval zebrafish. J Comp Neurol 501:1–12.

Ong CHP, Bateman A. 2003. Progranulin (Granulin-epithelin precursor, PC-cell derived growth factor, Acrogranin) in proliferation and tumorigenesis. Histology and Histopathology:1–14.

Otteson DC, D'Costa AR, Hitchcock PF. 2001. Putative Stem Cells and the Lineage of Rod Photoreceptors in the Mature Retina of the Goldfish. Developmental Biology 232:62–76.

Parichy DM, Ransom DG, Paw B, Zon LI, Johnson SL. 2000. An orthologue of the kit-related gene fms is required for development of neural crest-derived xanthophores and a subpopulation of adult melanocytes in the zebrafish, Danio rerio. Development 127:3031–3044.

Peri F, Nüsslein-Volhard C. 2008. Live Imaging of Neuronal Degradation by Microglia Reveals a Role for v0-ATPase a1 in Phagosomal Fusion In Vivo. Cell 133:916–927.

Philips T, De Muynck L, Thu HNT, Weynants B, Vanacker P, Dhondt J, Sleegers K, Schelhaas HJ, Verbeek M, Vandenberghe R, Sciot R, Van Broeckhoven C, Lambrechts D, Van Leuven F, Van Den Bosch L, Robberecht W, Van Damme P. 2010. Microglial upregulation of progranulin as a marker of motor neuron degeneration. J Neuropathol Exp Neurol 69:1191–1200.

Pickford F, Marcus J, Camargo LM, Xiao Q, Graham D, Mo JR, Burkhardt M, Kulkarni V, Crispino J, Hering H, Hutton M. 2011. Progranulin Is a

Chemoattractant for Microglia and Stimulates Their Endocytic Activity. AJPA 178:284–295.

Pixley FJ. 2012. Macrophage Migration and Its Regulation by CSF-1. International Journal of Cell Biology 2012:1–12.

Polazzi E, Contestabile A. 2002. Reciprocal interactions between microglia and neurons: from survival to neuropathology. Rev Neurosci 13:221–242.

Prinz M, Priller J. 2014. Microglia and brain macrophagesin the molecular age: from origin toneuropsychiatric disease. Nature Publishing Group 15:300–312.

QUASTLER H, SHERMAN FG. 1959. Cell population kinetics in the intestinal epithelium of the mouse. Exp Cell Res 17:420–438.

Rachel RA, Dölen G, Hayes NL, Lu A, Erskine L, Nowakowski RS, Mason CA. 2002. Spatiotemporal features of early neuronogenesis differ in wild-type and albino mouse retina. Journal of Neuroscience 22:4249–4263.

Raymond PA, Barthel LK, Bernardos RL, Perkowski JJ. 2006. Molecular characterization of retinal stem cells and their niches in adult zebrafish. BMC Dev Biol 6:36.

Ribeiro Xavier AL, Kress BT, Goldman SA, Lacerda de Menezes JR, Nedergaard M. 2015. A Distinct Population of Microglia Supports Adult Neurogenesis in the Subventricular Zone. Journal of Neuroscience 35:11848–11861.

Rossi F, Casano AM, Henke K, Richter K, Peri F. 2015. The SLC7A7 Transporter Identifies Microglial Precursors prior to Entry into the Brain. Cell Rep 11:1008–1017.

Ryan CL, Baranowski DC, Chitramuthu BP, Malik S, Li Z, Cao M, Minotti S, Durham HD, Kay DG, Shaw CA, Bennett HP, Bateman A. 2009. Progranulin is expressed within motor neurons and promotes neuronal cell survival. BMC Neurosci 10:130.

Saijo K, Glass CK. 2011. Microglial cell origin and phenotypes in health and disease. Nature Reviews Immunology 11:775–787.

Sato K. 2015. Effects of Microglia on Neurogenesis. Glia.

Schmitt EA, Dowling JE. 1994. Early eye morphogenesis in the zebrafish, Brachydanio rerio. J Comp Neurol 344:532–542.

Schmitt EA, Dowling JE. 1996. Comparison of topographical patterns of ganglion and photoreceptor cell differentiation in the retina of the zebrafish, Danio rerio. J Comp Neurol 371:222–234.

Schmitt EA, Dowling JE. 1999. Early retinal development in the zebrafish, Danio rerio: light and electron microscopic analyses. J Comp Neurol 404:515–536.

Schulte-Merker S, Stainier DYR. 2014. Out with the old, in with the new: reassessing morpholino knockdowns in light of genome editing technology. Development 141:3103–3104.

Schwarz JM, Bilbo SD. 2013. Microglia and Neurodevelopment: Programming of Cognition throughout the Lifespan. The Wiley-Blackwell Handbook of ….

Shiau CE, Monk KR, Joo W, Talbot WS. 2013. An anti-inflammatory NOD-like receptor is required for microglia development. Cell Rep 5:1342–1352.

Shigemoto-Mogami Y, Hoshikawa K, Goldman JE, Sekino Y, Sato K. 2014. Microglia Enhance Neurogenesis and Oligodendrogenesis in the Early Postnatal Subventricular Zone. Journal of Neuroscience 34:2231–2243.

Su P, Zhang J, Zhao F, Aschner M, Chen J, Luo W. 2014. The interaction between microglia and neural stem/precursor cells. Brain Res Bull 109:32–38.

Swamydas M, Nguyen D, Allen LD, Eddy J, Dréau D. 2011. Progranulin stimulated by LPA promotes the migration of aggressive breast cancer cells. Cell Commun Adhes 18:119–130.

Swinnen N, Smolders S, Avila A, Notelaers K. 2013. Complex invasion pattern of the cerebral cortex bymicroglial cells during development of the mouse embryo. Glia.

Tangkeangsirisin W. 2004. PC cell-derived growth factor (PCDGF/GP88, progranulin) stimulates migration, invasiveness and VEGF expression in breast cancer cells. Carcinogenesis 25:1587–1592.

Taylor SM, Alvarez-Delfin K, Saade CJ, Thomas JL, Thummel R, Fadool JM, Hitchcock PF. 2015. The bHLH Transcription Factor NeuroD Governs Photoreceptor Genesis and Regeneration Through Delta-Notch Signaling. Invest Ophthalmol Vis Sci 56:7496–7515.

Van Damme P, Van Hoecke A, Lambrechts D, Vanacker P, Bogaert E, van Swieten J, Carmeliet P, Van Den Bosch L, Robberecht W. 2008. Progranulin functions as a neurotrophic factor to regulate neurite outgrowth and enhance neuronal survival. J Cell Biol 181:37–41.

Verney C, Monier A, Fallet-Bianco C, Gressens P. 2010. Early microglial colonization of the human forebrain and possible involvement in periventricular white-matter injury of preterm infants. J Anat 217:436–448.

Walton NM, Sutter BM, Laywell ED, Levkoff LH, Kearns SM, Marshall GP, Scheffler B, Steindler DA. 2006. Microglia instruct subventricular zone neurogenesis. Glia 54:815–825.

Wang M, Li G, Yin J, Lin T, Zhang J. 2011. Progranulin overexpression predicts overall survival in patients with glioblastoma. Med Oncol.

Westerfield, Monte. The Zebrafish Book: A Guide for the Laboratory Use of Zebrafish (Danio Rerio) 4th edition, University of Oregon Press, Eugene, OR

Youn BS, Bang SI, Kloting N, Park JW, Lee N, Oh JE, Pi KB, Lee TH, Ruschke K, Fasshauer M, Stumvoll M, Bluher M. 2009. Serum Progranulin Concentrations May Be Associated With Macrophage Infiltration Into Omental Adipose Tissue. Diabetes 58:627–636.

Zhou J, Gao G, Crabb JW, Serrero G. 1993. Purification of an autocrine growth factor homologous with mouse epithelin precursor from a highly tumorigenic cell line. J Biol Chem 268:10863–10869.